Collection de notes internes de la Direction des Etudes et Recherches

VIEILLISSEMENT THERMIQUE ENTRE 300 ET 400°C D'ACIERS INOXYDABLES AUSTENOFERRITIQUES MOULES.

THERMAL AGEING OF DUPLEX STAINLESS STEELS

EDF
Electricité de France

EDF
Electricité de France

Direction des Etudes et Recherches

SERVICE RÉACTEURS NUCLÉAIRES ET ECHANGEURS
Département Etude des Matériaux

Mars 1992

MASSOUD J.P.
VAN DUYSEN J.C.
ZACHARIE G.

VIEILLISSEMENT THERMIQUE ENTRE 300 ET 400°C D'ACIERS INOXYDABLES AUSTENOFERRITIQUES MOULES.

THERMAL AGEING OF DUPLEX STAINLESS STEELS

Pages : 27

93NB00024

Diffusion : J.-M. Lecœuvre
EDF-DER
Service IPN. Département SID
1, avenue du Général-de-Gaulle
92141 Clamart Cedex

ISSN 1161-0611

SYNTHÈSE :

L'évolution des propriétés mécaniques de deux aciers inoxydables austénoferritiques moulés a été étudiée en relation avec l'évolution de leur microstructure après vieillissements de longues durées entre 300 et 400°C. La démixtion de la solution solide ferritique Fe-Cr-Ni par décomposition spinodale et la précipitation de phases intermétalliques sont les principales caractéristiques de cette évolution structurale.

EXECUTIVE SUMMARY :

The evolution of the mechanical properties of Mobearing and Mo-free cast duplex stainless steels, induced by long term ageing in the range 300-400°C, has been studied in relation with the evolution of their microstructure. The unmixing of the ferritic Fe-Cr-Ni solid solution by three-dimensional (sponge-like) spinodal decomposition and the precipitation of intermetallic G-phase particles are the main characteristics of this microstructural evolution.

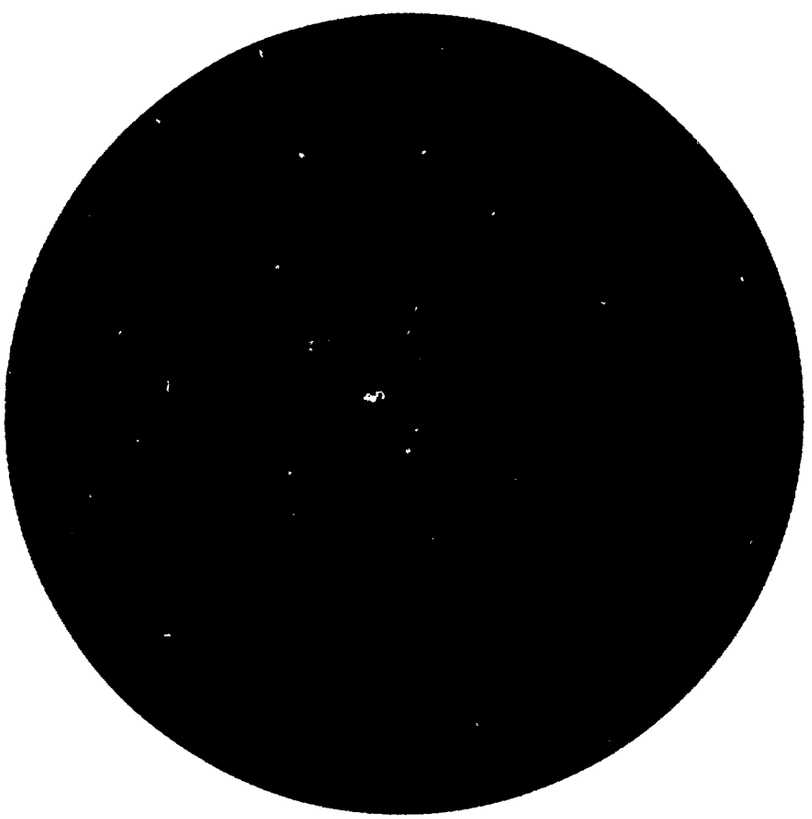

THERMAL AGEING OF DUPLEX STAINLESS STEELS

J. P. MASSOUD, J.C. VAN DUYSEN, G. ZACHARIE
Electricité de France, DER/EMA 77250 Moret sur Loing

P. AUGER*, F. DANOIX*
* URA, CNRS, 808 UFR Sciences, Université de Rouen 76130 Mont Saint Aignan

1 - Introduction :

Some components of the primary loop of pressurised water reactors are made of cast duplex stainless steel (austenite + ferrite). This kind of steel may age even at relatively low temperatures (i. e. under 400°C) due to a microstructural evolution of the ferritic phase (well known as the "475°C embrittlement").

Because of the risk of ageing of these components in the temperature range of service conditions (i. e. around 300°C), many efforts have been devoted by EDF to this problem over the last 10 years. The behaviour of a wide variety of duplex stainless steels ("Mo-bearing" and "Mo-free" grades ; the so called Mo-free heats contain in fact a small amount of molybdenum) from various steelmakers has been studied upon prolonged thermal ageing. This work essentially consists in monitoring the evolution of mechanical properties (tensile, hardness, impact and fracture toughness) (1) and of the microstructure (2). We have the double aim of understanding the influence of metallurgical parameters upon ageing behaviour and establishing extrapolation methods to evaluate the end of life properties.

2 - Materials studied. Mechanical tests and examination performed :

A wide variety of materials has been investigated by EDF (1), including Mo-bearing and Mo-free heats from various steelmakers. Their chemical composition and ferrite content (table 1) cover the entire specified ranges for french PWRs in order to gain some insight into in service behaviour of real components. Furthermore, some materials are out

of the specified chemical composition and ferrite content so that extreme ageing behaviour can be tentatively assessed.

Up to now, ageing treatments have been carried out at 300, 325, 350 and 400°C for times up to 30 000 h, longer ones are under way to reach 100 000 h. The wide studied temperature range not only allows to cover the real service conditions (285-325°C) but also provides "accelerated" ageing data which may be used for extrapolation to low temperatures.

We have mainly characterised the ageing behaviour of the studied material through the evolution of hardness, Charpy U-notch impact toughness at room temperature and Charpy V-notch impact toughness at 320°C. So, only these mechanical properties will be discussed.

Microstructural investigations have been essentially performed on the A10 "Mo-bearing" heat and the A'2 "Mo-free" heat (table 1).

3 - Evolution of mechanical properties as a function of metallurgical and ageing parameters :

As-received conditions

Let us first consider the influence of metallurgical parameters on the toughness. Some 320°C Charpy V-notch impact toughness values (corresponding to the upper shelf energy : USE) determined upon Mo-free and Mo-bearing steels from several steelmakers are plotted on figure 1. It is apparent that the upper shelf Charpy energy in as-received conditions is quite variable and is not simply correlated with the measured ferrite content. The results are identical for the Charpy U-notch toughness at 20°C (corresponding also to the USE).

Conversely, USE is better correlated with the Cr+Mo+Si content (or chromium equivalent, Cr*, i. e. total amount of ferrite forming elements) of those materials (figure 2). USE is also correlated with nickel content because Cr* and Ni contents are not fully independant so as to control the ferrite content.

Contrary to toughness properties, hardness (HV30) in as-received conditions is more dependant upon ferrite content than upon equivalent chromium content (figure 3). HV30 is simply related to the ferrite content (δ) according to the equation : $HV30=147+1.5\delta$. Microhardness (HV0.05) of the ferrite is larger in Mo-bearing than in Mo-free heats but is not significantly different among the various heats of a same grade (1).

After ageing

After ageing, a wide variety of behaviour is observed. In particular, a considerable difference exists between Mo-bearing and Mo-free grades with equivalent ferrite contents after ageing at 350°C. This phenomenon is for instance shown with the Charpy U-notch impact toughness on figure 4. It has been partly attributed to an effect of Mo. However the addition of this element is in general compensated by an increase in Ni content (in order to control the ferrite content) ; so the effect of Ni must also be considered.

It appears on figure 4 that the embrittlement of Mo-bearing steels is equivalent after ageing at 350°C and 400°C, and sometimes even more severe

after ageing at 350°C (1). The phenomenon is not observed for Mo-free grades. These results suggest that the embrittlement has a C-curve kinetic, the nose of which is lower (below 400°C) for Mo-bearing grade than for Mo-free grade. This behaviour implies that, at least for Mo-bearing steels, it is difficult to use the 400°C data to make extrapolations to lower temperatures.

For both Mo-free and Mo-bearing, the 320°C impact toughness after ageing steadily decreases when ageing temperature or time increase. This is consistant with the evolution of hardness which increases with these ageing parameters (1).

We have tried to correlate the room temperature or 320°C impact toughness after ageing with metallurgical parameters. It is difficult to find a simple correlation between these mechanical properties and the ferrite content.This can be observed on figure 5 where the 320°C impact toughness after ageing 30 000 h at 350°C has been plotted versus the ferrite content. A large scattering is observed particularly for ferrite contents below 17 % (in this range of low ferrite contents, different types of solidification can occur, inducing different types of morphology). However there is a good correlation between impact toughness at 320°C and equivalent chromium (Cr+Mo+Si) content, irrespective of the ferrite content (figure 6).

As in unaged conditions, hardness after ageing mainly depends on ferrite content (figure 3). The hardness after ageing could be expressed in function of ferrite content by the equation HV30=147+K.δ(%) where K depends on ageing conditions.

4 - Microstructural evolution - Mechanisms of embrittlement :

Among the numerous materials, the mechanical propreties of which have been studied, a Mo-bearing (A10) and a Mo-free (A'2) steel have been chosen to study the effects of ageing on the microstructure (table 2). The A10 steel is far more susceptible to ageing than A'2.

The microstructural evolutions have been studied mainly by Transmission Electron Microscopy (TEM) at EDF, by Atom Probe and Field Ion Microscopy (APFIM) at University of Rouen and (in a preliminary work) by Small Angle Neutron Scattering (SANS) at Institut Laue langevin.

It is now well known that the embrittlement during ageing (T<475°C) of duplex stainless steels is basically due to the microstructural evolution of the ferritic phase. Only minor evolutions (without hardening effect), if any, take place in the austenite. The main microstructural evolution in the ferrite are the unmixing of the ferritic Fe-Cr solid solution and the precipitation of intermetallic compounds.

Unmixing of the ferritic Fe-Cr solid solution

The ferrite of duplex stainless steels is unstable at intermediate temperatures and may decompose into Fe-rich α and Cr-rich α' domains by spinodal decomposition (in interconnected 3-dimensional networks : sponge-like) or precipitation (nucleation and growth). Other alloying elements segregate too but to a lesser extent : Mo to α' and Ni to α.

Because of its high spatial resolution, the atom-probe is an attractive tool for the investigation of this fine-scale decomposition. The analysed volume in the specimen is a cylinder, the diameter of which (lateral resolution) is 1nm. Concentration profiles can be constructed atomic layer after atomic layer.

For the Mo-bearing heat (A10), figure 7 shows Cr-concentration profiles and related concentration frequency distributions for several ageing treatments. As ageing proceeds, Cr-rich and Cr-poor zones appear. Concomitantly the concentration frequency distribution broadens and differs more and more from the random distribution observed in as quenched samples. This evolution can be followed with a statistical parameter called the Variation (V) (it is the integral of the difference between the Cr-concentrations frequency distribution of the aged sample and the random distribution [3]). This parameter reflects the amplitude of fluctuations and directly accounts for the evolution of the unmixing process. Its value may increase from 0 to 2 when the unmixing proceeds. Results obtained for different ageing treatments are reported table 3. Between 300 and 400°C, both the amplitude ΔC and the wavelength λ of the fluctuations in the ferrite increase with ageing time and temperature, indicating a spinodal decomposition. At the lowest temperatures, 300 and 350°C (for t<2500 h), the Cr concentration profiles can be described in terms of sinusoids, consistently with classical models for spinodal decomposition. Identical results have been obtained on heat A'2. The problem increases in complexity when ageing proceeds at 400°C or during long time at 350°C. As the concentration histograms tend towards a bimodal distribution, long range fluctuations emerge and increase in amplitude with ageing time. At least three different scales of distances are visible, leading to a structure with internal selfsimilarity as shown on figure 8.

As the properties of such a complex structure may not depend only on amplitudes but also on the detailled topology, it should be of prime interest to characterize the microstructure in terms of percolation, connectivity and fractal dimension. A complete morphological exploration of the sponge-like structure will soon be accessible with the new generation of 3-D atom-probes (4).

Some preliminary experiments have been attempted with SANS on the same heats A10 and A'2, in order to obtain additional informations concerning the fine scale microstructure (5). The SANS measurements have been performed on the two heats in the as-received conditions and after ageing at 300, 350 and 400°C for various times. The scattering patterns (figure 9) are characterized by the emergence (after ageing only) of an interference peak which grows in intensity and shifts toward smaller scattering vector values ($K=4x\Pi x\sin\theta/\lambda$, where θ is the diffusion angle and λ the wavelength of neutron beam) as ageing time progresses. It reveals a nonrandom distribution of two phases (apparently α-α' unmixing). Models have to be used to deduce metallurgical parameters (interphase distances, volume fraction of precipated phase ...) from these scattering patterns.

Precipitation of intermetallic phases in the ferrite

Concomitantly with the spinodal decomposition, a precipitation of small intragranular quasi spherical particles of G-phase (type $Ni_{16}Ti_6Si_7$ where Cr, Fe, Mo, Mn can substitute to Ti and Ni) has been observed in the studied materials. The density of these precipitates is much higher in the Mo-bearing than in the Mo-free steels (figure 10) (2).

Atom probe experiments reveal that (2) the G-phase particles, except the largest ones (which grow on dislocations), systematically develop at α-α' "interfaces" (figure 11). This location is apparently due to preferential rejection of supersaturated Ni and Si from Cr-rich and Fe-rich domains respectively. The opposite fluxes of both species facilitate the nucleation and growth of the new phase at the α-α' "interface" since it is particularly rich in Ni and Si. Thus G-phase precipitation is driven by spinodal decomposition. However, extensive α-α' unmixing is observed without any (or with only small amounts) G particles in the Mo-free steel, and in the first stages of ageing of the Mo-bearing steel.

The G-phase precipitation in the temperature range 300-400°C is a generic appellation which covers different stages in the evolution from Ni-Si clusters to a complex steady state. The size of these particles remains small even after long term ageing treatment at 350°C (table IV). These particles are enriched in all alloying elements except Fe and Cr (figure 12). They exhibit some internal segregation may be related to their presence at the α-α' "interface". Opposition between Mn and Mo, Al and Mo, as well as attraction between C and Mo, can be pointed out (figure 12).

5 - Relationship between microstructural evolution during ageing and mechanical properties

The evolution of the ferrite hardness (measured by microhardness tests) with the ageing time at 300 and 350°C can be accounted for in terms of increasing Cr-amplitude (ΔC) measured by mean of atom-probe (figure 13a). The observed linear relationship between $HV_{0.05}$ and ΔC may result from a hardening mechanism based on a α-α' misfit inducing an elastic stress (14). The correlation can not be extended to 400°C because of a change in decomposition morphology which preclude ΔC to be defined. However, using the V parameter, a very good correlation was obtained between microstructural evolution and ferrite hardening in the temperature range 300-400°C (figure 13b) (indicating that this integral parameter is pertinent).

The activation energies for ferrite hardening and for spinodal decomposition are consistant in the range 300-400°C and quite close to that for Cr-diffusion in α-iron (i.e. about 250 kJ/mole) (6). However, from the kinetics of macroscopic mechanical properties (toughness or macrohardness), it has been shown that there is no single "apparent activation energy" (evaluated from T^{-1} versus lnt plots of isotoughness curves) in the range 300-400°C, but several apparent activation energies the values of which increase with decreasing temperature (1). At lower temperatures (i. e. close to in service temperature), this energy is about 250 kJ/mole, which is in good agreement with that of the spinodal decomposition. The high discrepancy at higher temperatures (T>350°C) suggests that a change takes place in the mechanisms of macroscopic mechanical deformation and fracture. In that case, the decrease of toughness does not depend only on ferrite unmixing any more.

Influence of alloying elements

Ni is claimed to accelerate the kinetics of spinodal decomposition of ternary Fe-Cr-Ni alloys (11, 12, 13). For the heats A10 and A'2 (table 5), the values of the parameter V (which increases as the Cr-concentration fluctuation amplitude ΔC rises) clearly show that the Mo-bearing steel (containing 6.1 at % Ni in the ferrite, table 2) decomposes more rapidly than the Mo-free steel (which contains only 4.7 at %, table 2). This difference in the α-α' decomposition kinetics may be attributed to the Ni-

content of the ferrite and can explain partly the more rapid decrease in toughness of the Mo-bearing steel. Nevertheless this difference alone is not sufficient to explain the considerable differences in embrittlement between the two steels. Indeed, for a given value of the V parameter (or ΔC), the associated hardening of the ferrite is higher for Mo-bearing than for Mo-free steels (table V). It is suggested that Mo atoms (preferentially located in α') enhances the elastic stress between α'Cr-rich domains and αFe-rich domains (figure 15)

Influence of G-phase

Spinodal decomposition is certainly the main hardening and embrittlement mechanism. Indeed, very good correlation have been obtained between the increase in hardness of ferrite and the increase in Cr concentration amplitude ΔC, both in the presence and absence (7-8) of G-phase. However it seems difficult to imagine that such a finely dispersed phase does not contribute to the hardening when its volume fraction reaches a few percent as it is the case in Mo-bearing steels. It is difficult to discriminate the contribution of G-phase from that of spinodal decomposition since precipitation kinetics depend on each others. It has been attempted to isolate these contributions with the help of reversion experiments, in with an aged material was reheated at 600°C, in order to dissolve the α and α' domains and not the G-phase (9, 10). The experiments have been performed on a material containing about 3% G-phase. It showed that the apparently complete suppression of the spinodal structure after reversion at 600°C did not restore the toughness and the hardness to their initial values. This may be due to the residual G-phase (figure 14).

6 - Fracture mechanisms

In the unaged conditions, the room temperature fracture is completely ductile with dimples (figure 16a). After ageing, the proportion of brittle fracture areas of ferrite increases (figure 16b). As shown on figure 16c, multiple and parallel cleavage of ferrite take place in the material. These cleavages appear firstly in ferrite grains, the crystallographic orientation of which is favourable with respect to the tensile axis. The proportion of brittle fracture can increase beyond that corresponding to the ferrite content (indicating that the embrittled ferrite becomes a preferential fracture path (1)). Finally it can even increase until the fracture apparence is almost completely brittle (figure 16d).

7 - Conclusions

The embrittlement of cast duplex stainless steels upon thermal ageing results from the microstructural evolution which takes place in the ferrite. The decrease in impact toughness of these materials is well correlated with the equivalent chromium content. This parameter is an indicator of both the ferrite content (which directly depends on this amount of ferrite forming elements) and of the amount of elements susceptible of enhancing the hardening of ferrite.

Investigation of the microstructural evolution of Mo-bearing and Mo-free duplex stainless steels upon long term ageing between 300 and 400°C have shown that the main microstructural changes are the unmixing of the ferritic Fe-Cr-Ni solid solution by three-dimensional (sponge-like) spinodal decomposition and the precipitation of intermetallic G-phase particles.

The evolution of the ferrite hardness (measured by microhardness) with ageing time can be accounted for in terms of increasing of spinodal parameters (ΔC or V). The hardening mechanism may be based on the α-α' misfit induced elastic strain. The activation energies for ferrite hardening and for spinodal decomposition are constant in the range 300-400°C and quite close to each other and to that of Cr diffusion in α-iron. However for the evolution of macroscopic mechanical properties (toughness or macrohardness) of the duplex steel, the activation energy decreases with increasing temperature which suggests a change in the mechanisms of macroscopic deformation of the duplex.

Mo-bearing heats (which also contain more nickel) are more sensitive to ageing at 350°C than Mo-free heats. It seems that, for a given Cr content, not only the Mo, but also the Ni concentration affect the decomposition. A given excess of Ni in the ferrite solid solution accelerates the spinodal decomposition and facilitates the nucleation and growth of the G-particles at α-α' "interfaces". It seems that Mo atoms (preferentially located in α') also enhance the elastic stress between α'-Cr rich domains and α-Fe rich domains and then increase the hardness of ferrite for a given spinodal decomposition.

8 - References

(1) BONNET et al., Mater. Sci. Technol., 6 (1990) p 221.
(2) AUGER et al., Mater. Sci. Technol., 6 (1990) p301.
(3) BLAVETTE et al., J. Phys., 49 C6 (1988) p 433.
(4) CEREZO et al., J. of Microscopy, 154, 3 (1989) p 215.
(5) EPPERSON et al., ASTM STP 955, 1987, p 595.
(6) GUTTMANN M., Int conf on Duplex Stainless Streels, 1991, Beaune, 28-30 octobre 1991, Editions de Physique, p 79.
(7) PUMPHREY et al., Mater. Sci. Technol., 6 (1990) p 211.
(8) BROWN et al., PVP ASME, 195 (1990) p 175.
(9) CHUNG H. M.,LEAX T. R.,Mater. Sci. Technol., 6 (1990) p 249.
(10) BOURGOIN J;, EDF /Dept EMA Intern Report n°HT-41/NTE 1053-A, Jul 1990
(11) SOLOMON H.D., LEVINSON L.M., Acta Met. 26 (1978) 429.
(12) COURTNAL M., PICKERING F.B., Met. Sci. 10 (1976) 276.
(13) HAYES F.H., HETHERINGTON M.G., Mater. Sci. Technol., 6 (1990) p 263.
(14) PARK K.H. et al., Acta Met., 34,(1986) 1853.

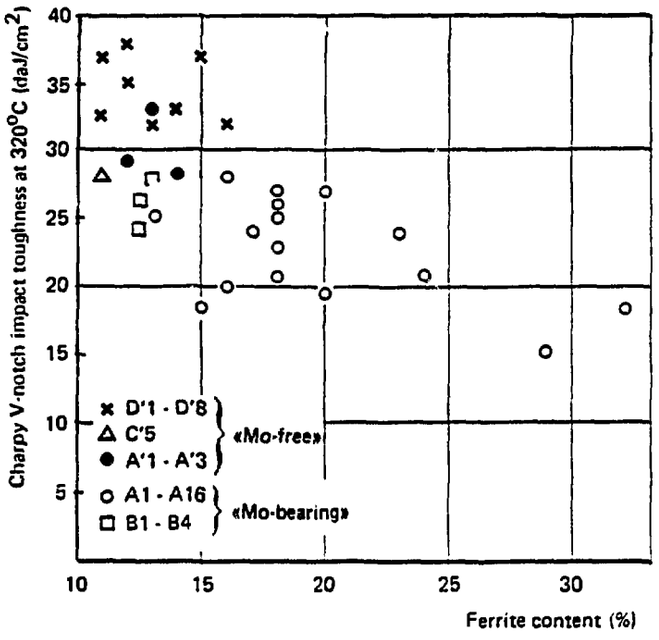

Figure 1 – Upper Shelf Energy as function of ferrite content.

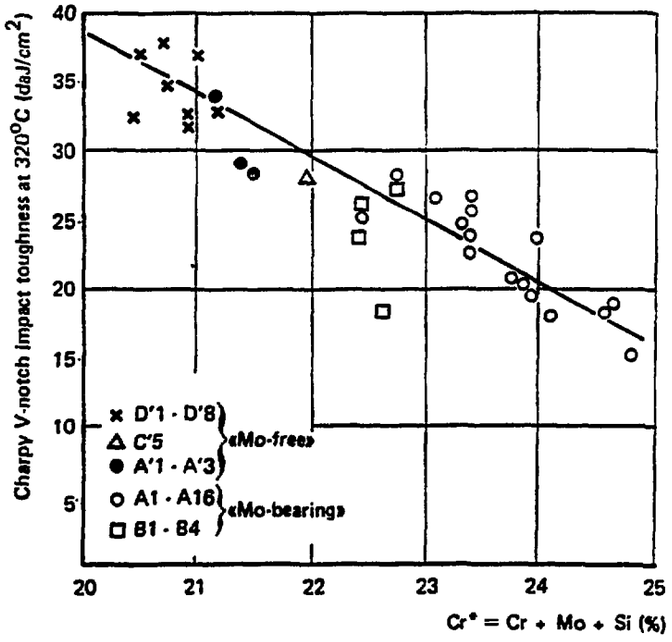

Figure 2 — Upper Shelf Charpy Energy as function of Cr* = Cr + Mo + Si contents of Mo-free and Mo-bearing heats in as received conditions.

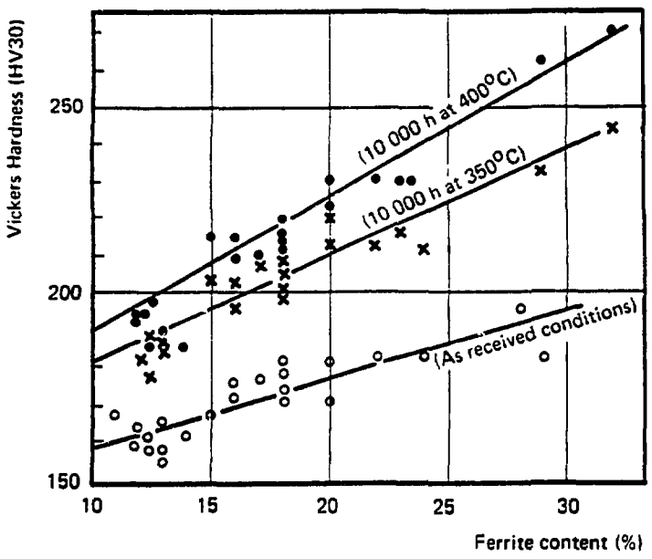

Figure 3 – Evolution of Hardness (HV30) with ferrite content in as-received conditions and after ageing for Mo-free and Mo-bearing heats.

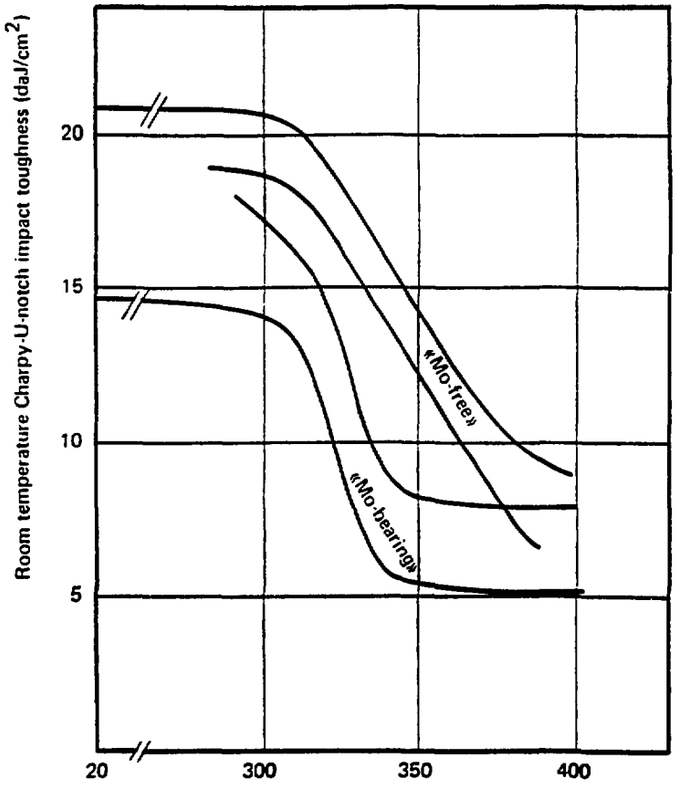

Figure 4 – Variation of room temperature Charpy-U-notch impact toughness of Mo-bearing (heats B1 to B4) and Mo-free (heats A'1 to A'3) heats with equivalent ferrite content as function of ageing temperature for 30 000 h aging.

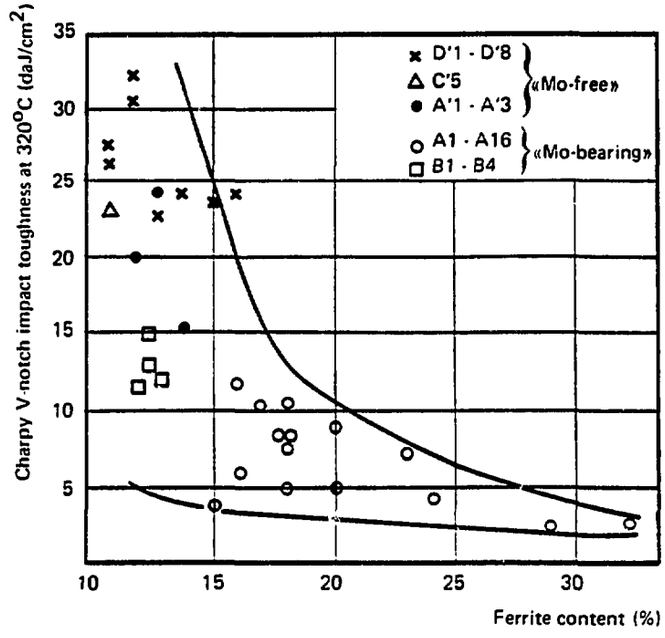

Figure 5 – Evolution of Charpy-V impact toughness at 320°C as function of ferrite content after aging 30 000 h at 350°C.

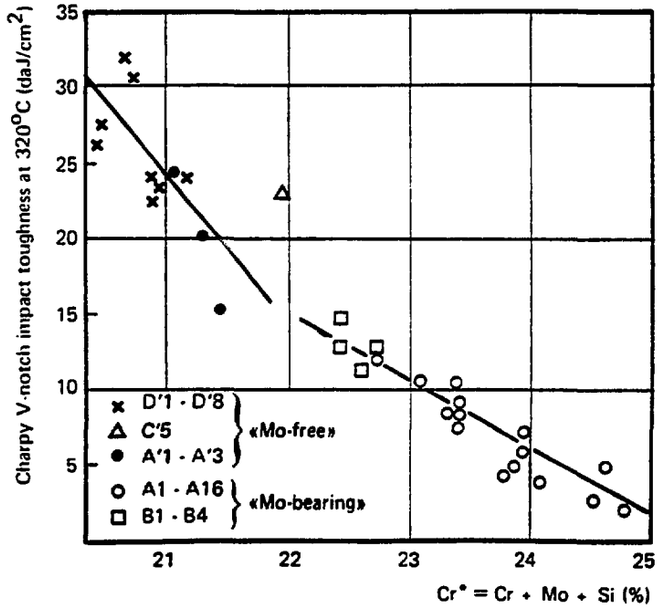

Figure 6 – Evolution of impact toughness at 320°C in function of Cr* = Cr + Mo + Si after aging 30 000 h at 350°C.

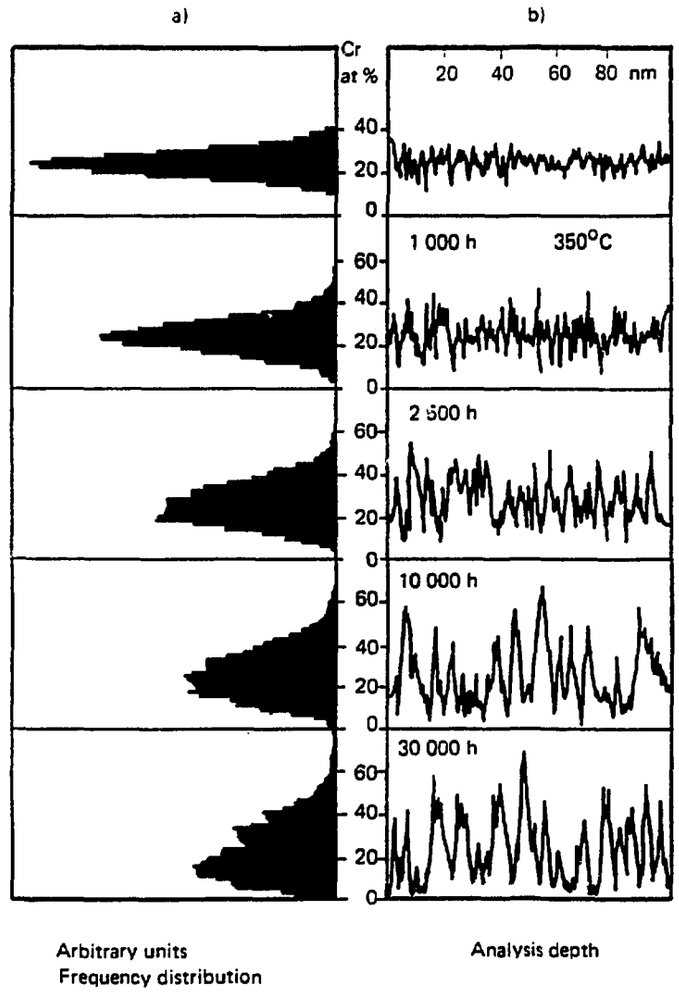

Figure 7 — Cr-concentration profiles (b) of the aged ferrite (350°C) and related Cr-concentration frequency distributions (a) (the frequency distribution is proportional to the number of times the corresponding concentration has been detected).

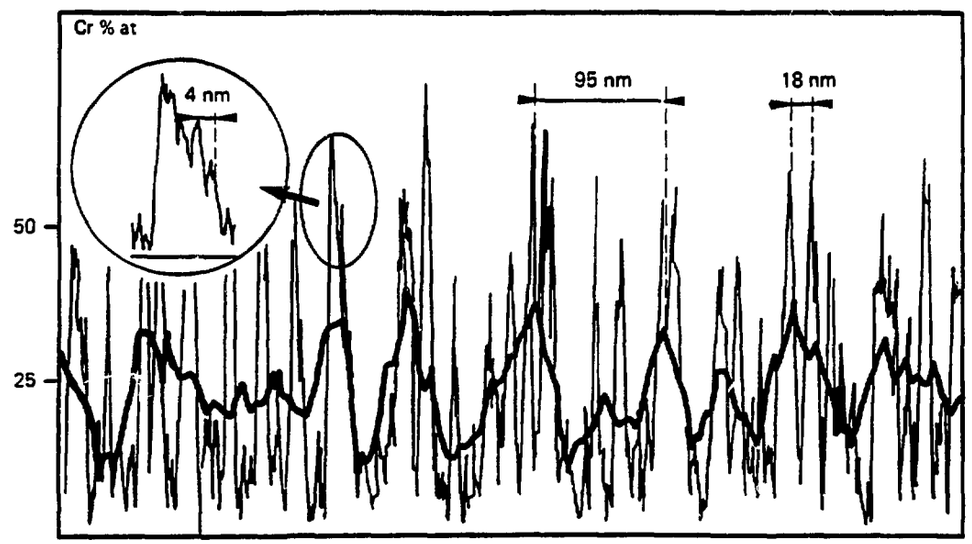

Figure 8 — Cr-concentration profiles (30 000 h at 400°C) exhibiting three different characteristic distances between chromium peaks. The three profiles have been drawn with different scales from the same set of experimental data.

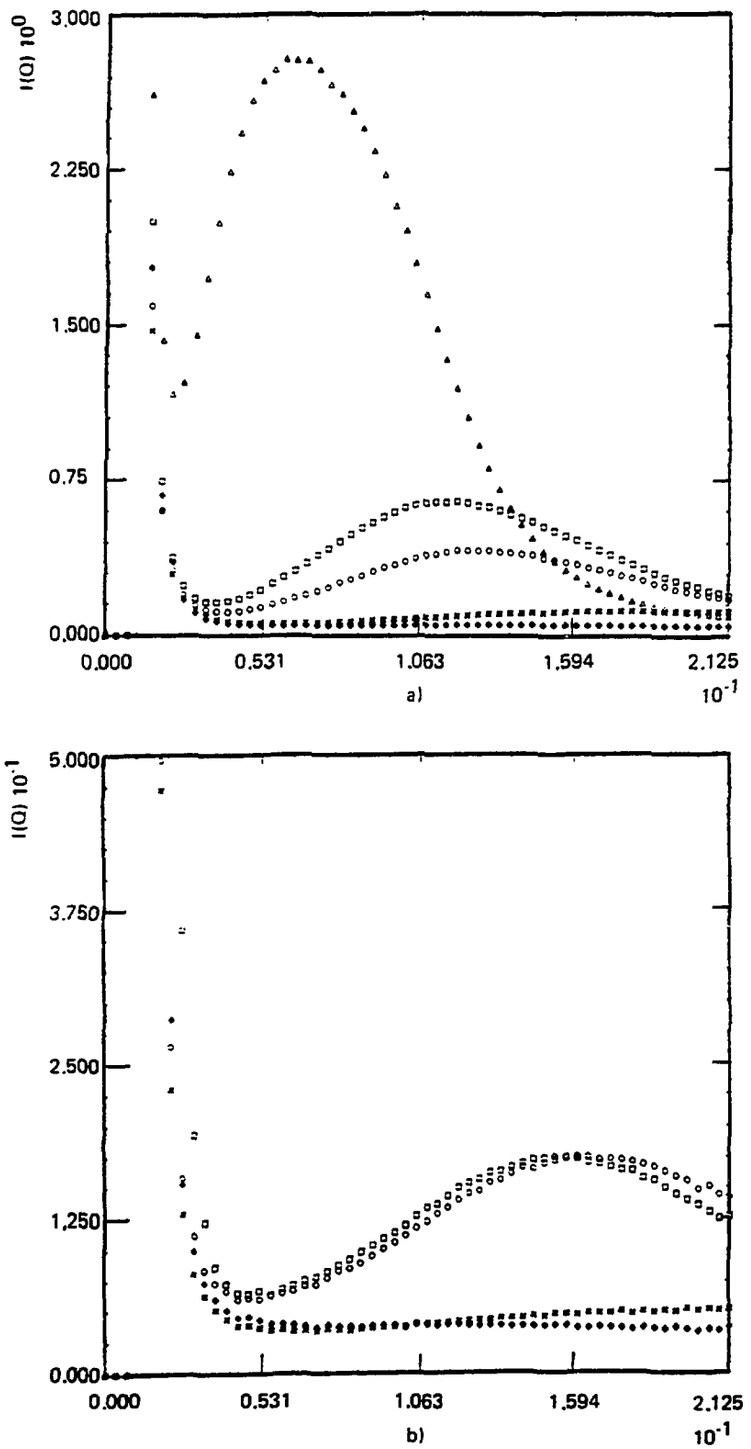

Figure 9 – Intensity I(k) vs wave vector $K = (2\pi \sin\theta)/\lambda$ plots fot heats A10 (a) and A'2 (b) in unaged conditions (+) and after ageing, 30 000 h 300°C (✱), 10 000 h 350°C (○), 30 000 h 350°C (□) and 30 000 h 400°C (△).

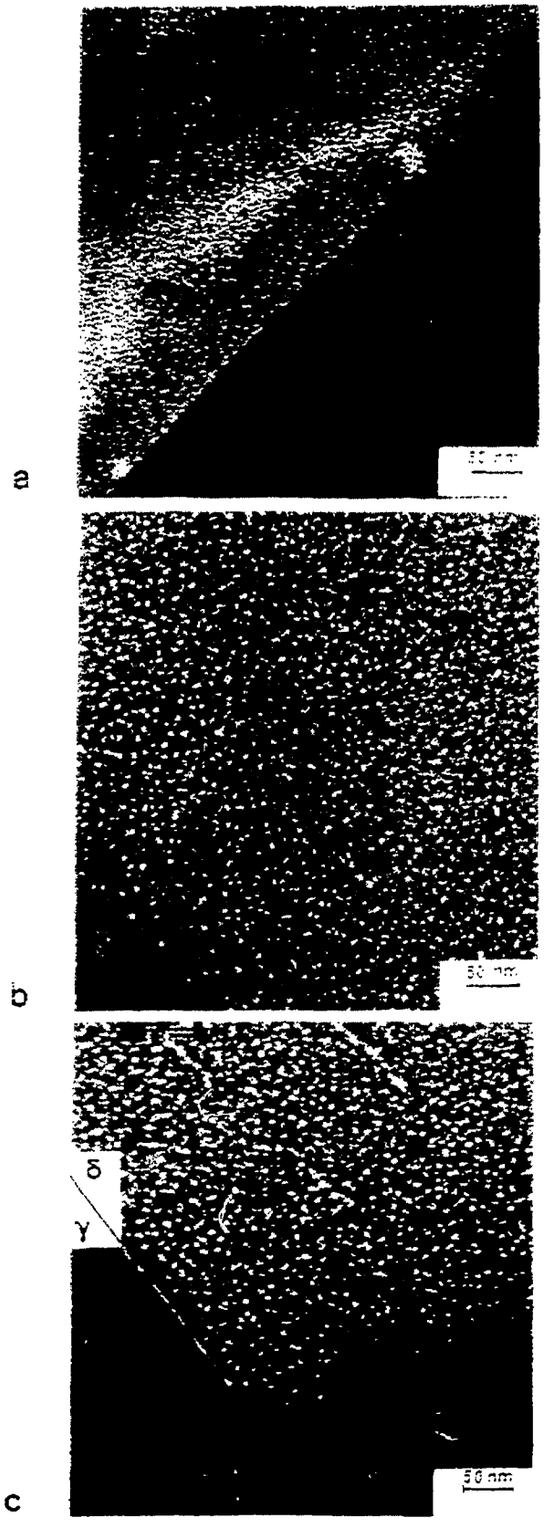

Fig.10 - Dark field images from $\{333\}_G$ showing G-phase size and distribution in heat A10 after ageing : (a) 350°C, 30 000 h ; (b) 400°C, 10 000 h and (c) 400°C, 30 000 h.

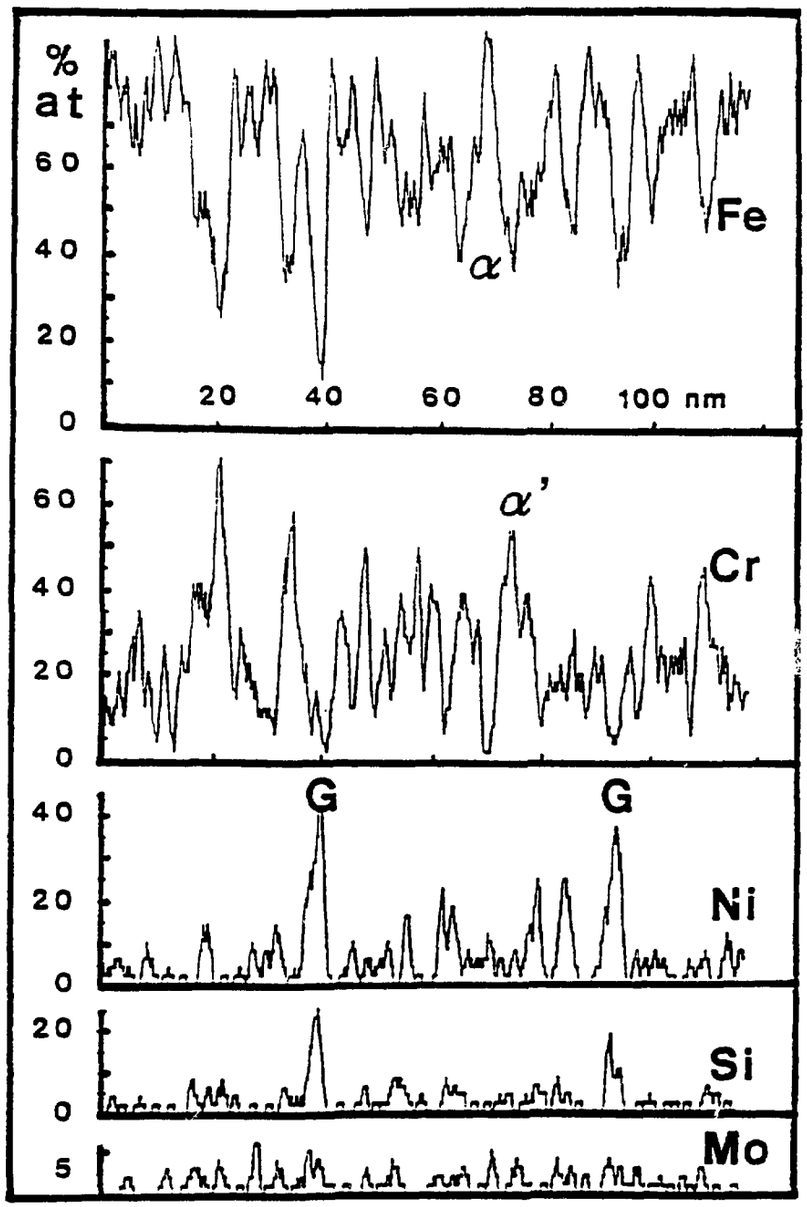

Figure 11. Concentration profiles (Mo-bearing steel A10 aged 30 000 h at 350°C) exhibiting Fe-rich α, Cr-rich α' domains and G-phase Ni-Si rich particles.

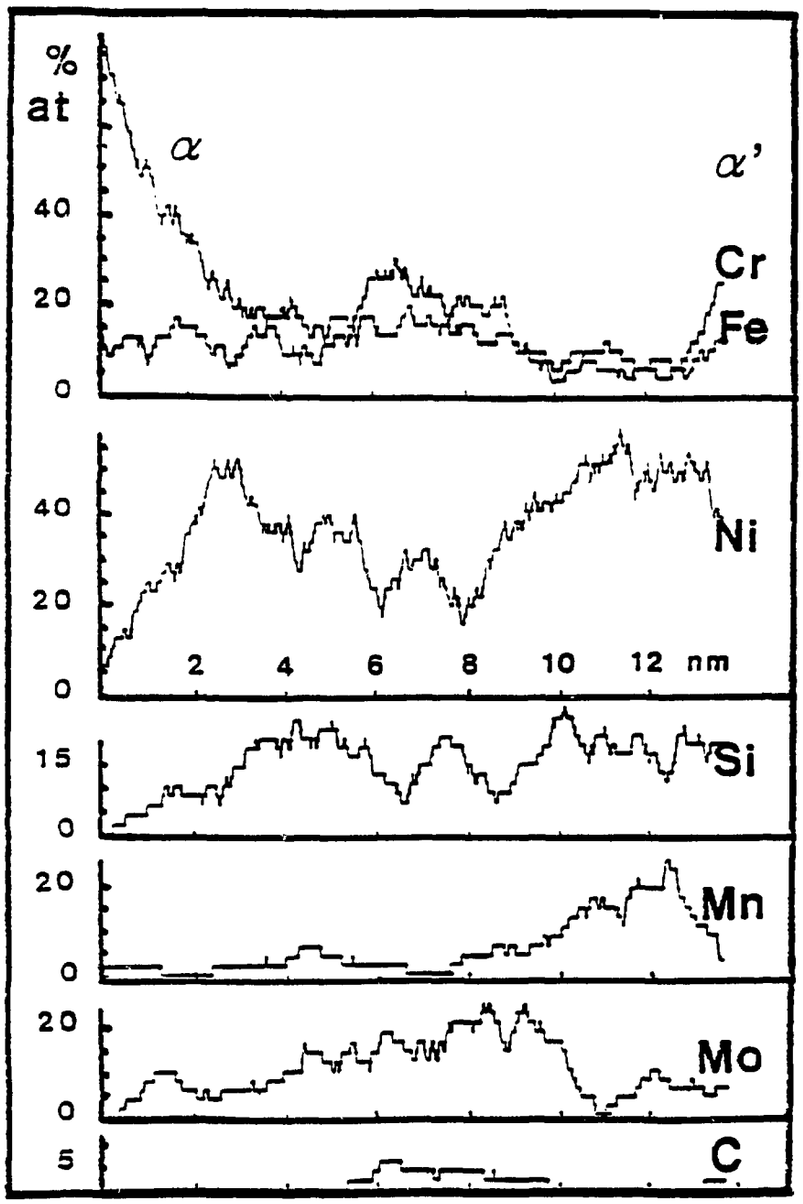

Figure12. Concentration profiles (Mo-bearing steel A10 aged 30 000 h at 400°C) across a complex "G-particle" showing the heterogeneous distribution of elements.

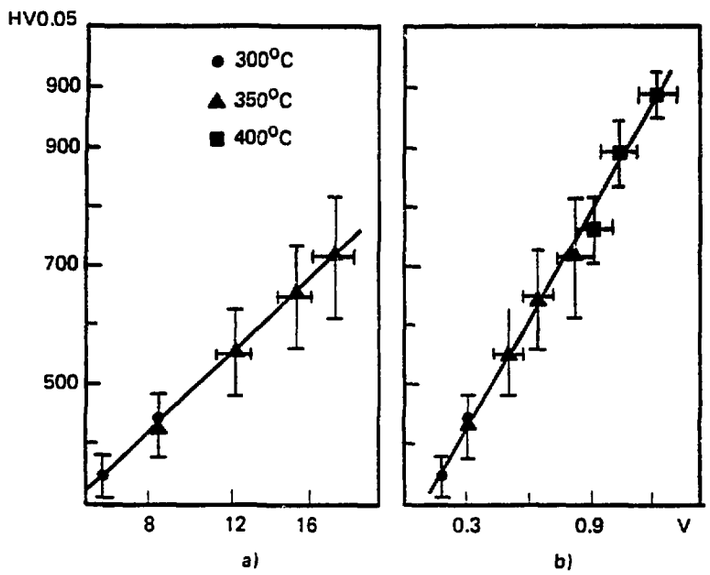

Figure 13 – Correlation between the ferrite microhardness HV0.05 of heat A10 and
a) the Cr fluctuation amplitude ΔC,
b) the microstructural parameter V.

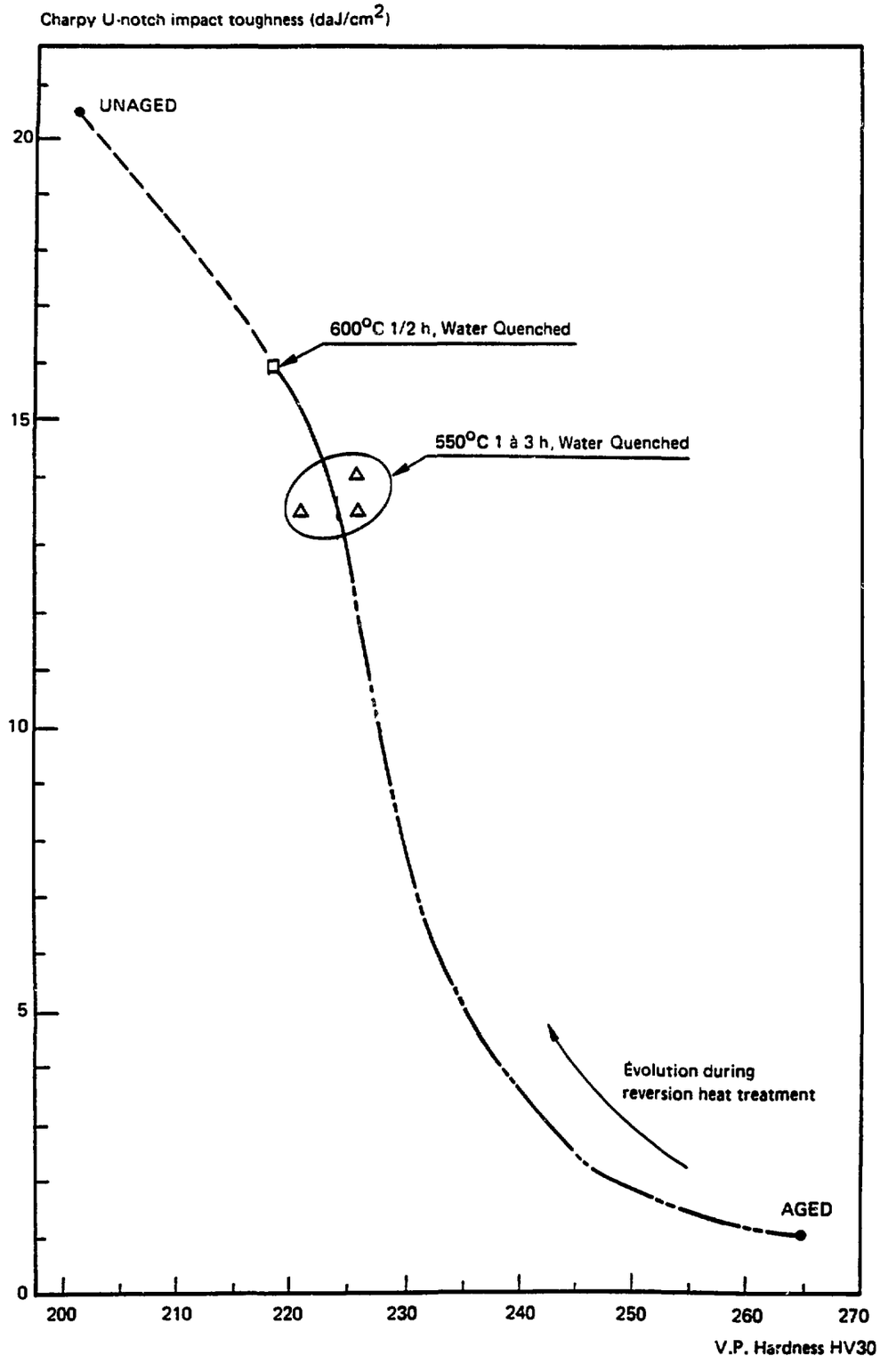

Figure 14 — Relations between hardness and Charpy-U impact toughness at room temperature in unaged conditions, after a 1000 h ageing at 400°C and after reversion experiments at 550 and 600°C [10].

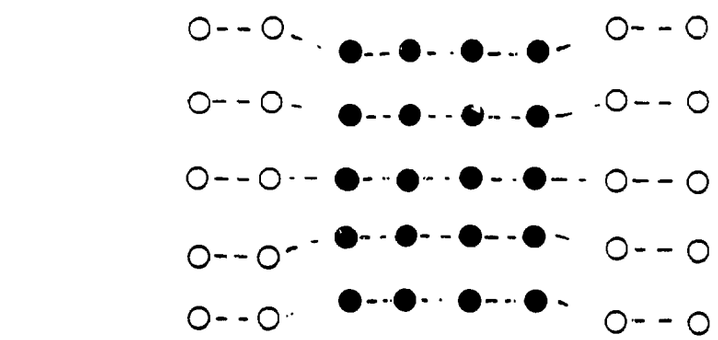

● Fe
○ Cr
✪ Mo

a - Mo-free materials

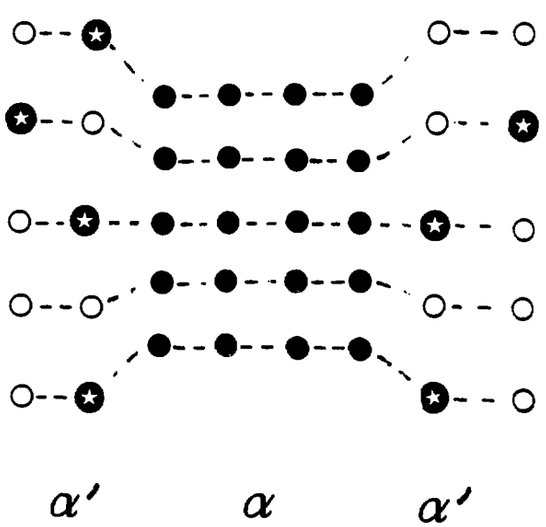

b - Mo-bearing materials

Figure 15 : Schematic effect of Mo-atoms (preferentially located in α') which enhance the elastic stress between α'Cr-rich and αFe-rich domains.

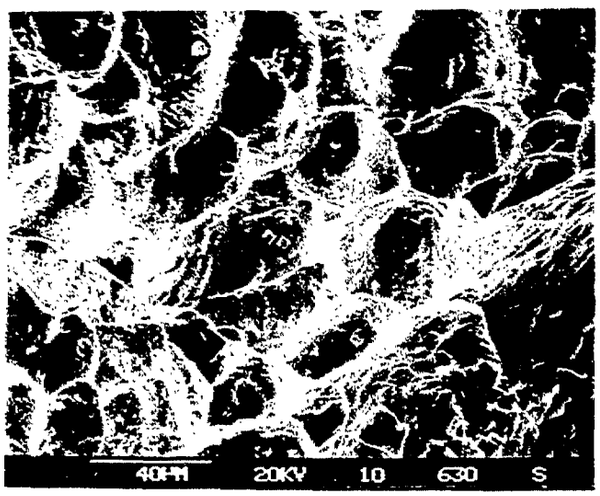

a –

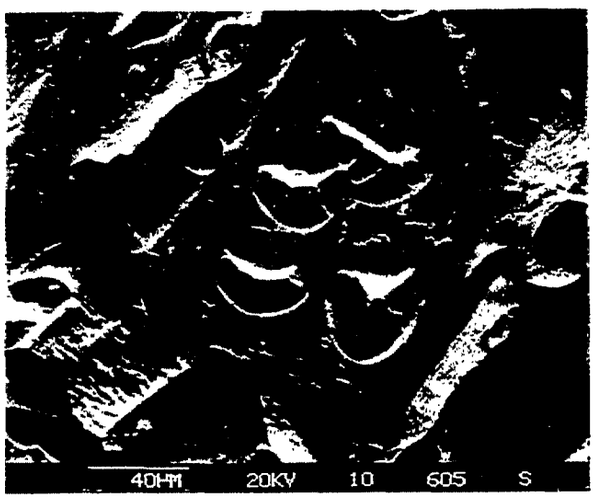

b –

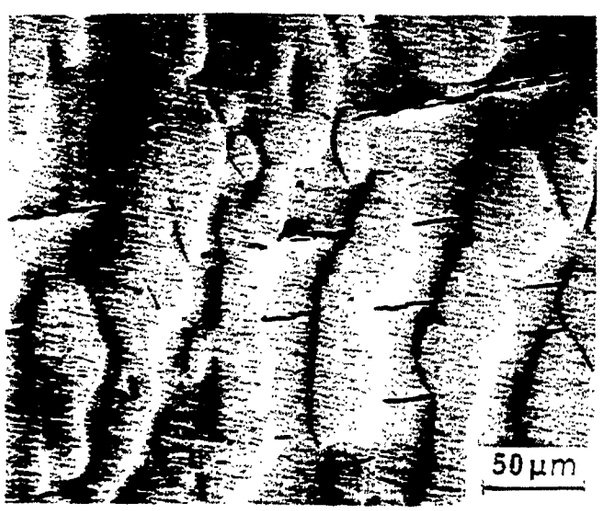

c –

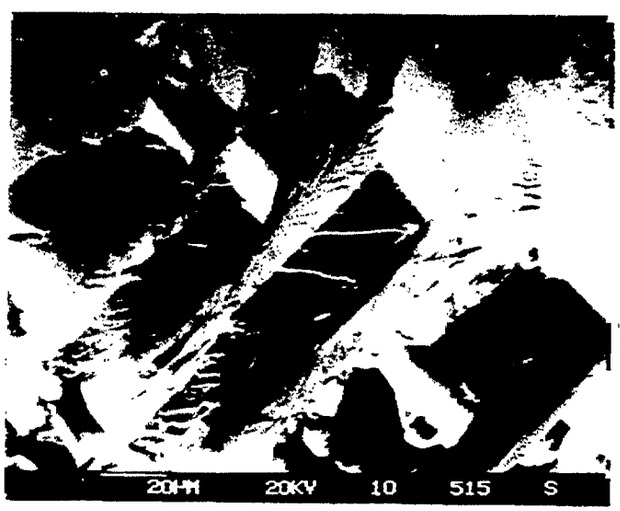

d –

Figure 16 : Aspects of damage at room temperature,
a) fracture surface in unaged conditions,
b) and d) fracture surface after ageing,
c) cleavage of ferrite in tensile testpieces strained to fracture

TABLE 1 – CHEMICAL COMPOSITION AND FERRITE CONTENT OF MATERIALS STUDIED.

Type of steel	Steel-maker	Type of casting*	Number of heats	Index of product	Chemical composition (wt.%)						Ferrite content (%)	
					C	Si	Mn	Ni	Cr	Mo	Schaeffler	Measured
Mo-bearing	A	S	16	A1 - A16	0.027 - 0.042	0.87 - 1.43	0.57 - 0.92	9.6 - 10.9	18.8 - 21.0	2.40 - 2.78	19 - 30	13 - 32
	B	S	4	B1 - B4	0.030 - 0.039	0.89 - 0.98	0.75 - 0.94	9.9 - 10.4	19.1 - 19.3	2.40 - 2.54	15 - 17	11 - 13
	C	S + C**	2	C1 - C4	0.038 - 0.050	1.17 - 1.21	0.68 - 0.80	10.2 - 10.4	20.6 - 22.2	2.58 - 2.75	20 - 34	20 - 34
	C	C	1	C5	0.020	0.99	0.70	10.6	19.3	2.38	17	10
Mo-free	A	S	3	A'1 - A'3	0.030 - 0.038	0.94 - 1.00	0.83 - 0.92	8.2 - 8.4	20.0 - 20.4	0.04 - 0.07	20 - 21	10 - 16
	B	S	4	B'1 - B'4	0.015 - 0.039	1.15 - 1.52	0.62 - 0.80	10.1 - 10.5	19.4 - 20.2	0.08 - 0.20	11 - 15	6 - 10
	C	S	4	C'1 - C'4	0.017 - 0.025	0.89 - 1.00	0.77 - 1.02	9.8 - 10.0	20.2 - 20.7	0.34 - 0.57	15 - 19	8 - 9
	C	C	1	C'5	0.034	1.04	0.62	9.0	20.7	0.17	19	11
	D	S	8	D'1 - D'8	0.018 - 0.029	0.71 - 0.86	0.39 - 0.44	8.2 - 8.5	19.4 - 19.9	0.24 - 0.39	19 - 24	11 - 16
	E	C	2	E'1 - E'2	0.034 - 0.056	1.02 - 1.18	0.71 - 0.76	8.0 - 8.4	20.6 - 20.8	0.02 - 0.05	22 - 26	13 - 21

* S : statically cast - C : centrifugally cast

**One S and one C product were made from each heat.

TABLE 2 – AVERAGE CHEMICAL COMPOSITIONS, FERRITE CONTENTS AND CHEMICAL COMPOSITIONS OF THE FERRITE (atom-probe).

	C	Si	Mn	Cr	Mo	Ni	Ferrite content
Steel A10 Average wt %	0.039	1.22	0.60	20.0	2.56	10.0	24 %
Ferrite A10 at %		2.8 ± 0.4	0.43 ± 0.10	24.0 ±1.5	2.2 ± 0.3	6.1 ± 1.0	
Steel A'2 Average wt %	0.038	0.94	0.83	20.4	0.07	8.4	14 %
Ferrite A'2 at %		2.3 ± 0.3	0.62 ± 0.05	26.0 ± 1.5	0.16 ± 0.03	4.7 ± 0.4	

TABLE 3 – EVOLUTION OF MICROSTRUCTURAL PARAMETERS V, ΔC, λ, AND FERRITE MICROHARDNESS HV0.05 FOR DIFFERENT AGEING TREATMENTS. HEAT (A10).

Ageing treatment	V	ΔC (at %)	λ (nm)	HV0.05
10 000 h 300°C	0.18 ± 0.03	5.9 ± 0.5	3.5 ± 1.0	348 ± 38
30 000 h 300°C	0.32 ± 0.05	8.4 ± 0.6	5.5 ± 1.0	450 ± 45
1 000 h 350°C	0.31 ± 0.05	8.7 ± 0.6	4.5 ± 1.0	435 ± 55
2 500 h 350°C	0.51 ± 0.07	12.6 ± 0.8	5.5 ± 1.0	553 ± 73
10 000 h 350°C	0.67 ± 0.07	15.6 ± 0.8	7.0 ± 1.5	648 ± 86
30 000 h 350°C	0.87 ± 0.08	17.4 ± 1.0	8.0 ± 2.0	716 ± 104
2 500 h 400°C	0.97 ± 0.09	⊗	⊗	763 ± 52
10 000 h 400°C	1.1 ± 0.1	⊗	⊗	890 ± 60
30 000 h 400°C	1.3 ± 0.1	⊗	⊗	989 ± 38

⊗ not determinable with a single value.

TABLE 4 – MICROSTRUCTURAL PARAMETERS : Φ_p PARTICLE DIAMETER, N_p PARTICLE DENSITY, f_v PARTICLE VOLUME FRACTION, C_G TOTAL CONTENT OF Ni, Si AND Mo OF THE G-PHASE. Mo-BEARING STEEL AGED AT 350°C.

	Φ_p (nm)	N_p (cm^{-3})	f_v (%)	C_G (at %)
1 000 h	4.0	$4.5.10^{17}$	1.5	40 ± 4
2 500 h	5.0	$6.5.10^{17}$	4.0	49 ± 4
10 000 h	6.0	$4.5.10^{17}$	5.0	47 ± 4
30 000 h	6.0	5.10^{17}	5.5	60 ± 4

TABLE 5 – PARAMETER, MICROHARDNESS OF FERRITE AND IMPACT TOUGHNESS VALUES. Mo-BEARING A10 AND Mo-FREE A'2 STEELS AGED 10 000 AND 30 000 H AT 350°C.

Aging treatment 350°C	V*	Room temperature toughness (daJ/cm^2)	HV0.05 (scattering)
Steel A'2 10 000 h	0.37	16	350 (54)
Steel A'2 30 000 h	0.66	12	439 (26)
Steel A10 10 000 h	0.52	3	648 (86)
Steel A10 30 000 h	0.83	2.5	716 (104)

*These measurements were exceptionally carried out with a variable lateral resolution ($1\ nm < \Phi_a < 3\ nm$).